PHYSICAL REVIEW E **95**, 012705 (2017)

Birefringence in the vicinity of the smectic-*A* to smectic-*C* phase transition: Crossover from *XY* critical to tricritical behavior

Malay Kumar Das,[1,*] Susanta Chakraborty,[1] Roman Dabrowski,[2] and Michał Czerwiński[2]
[1]*Department of Physics, University of North Bengal, Siliguri, Darjeeling 734 013, India*
[2]*Faculty of Advanced Technologies and Chemistry, Military University of Technology, Kaliskiego Street 2, 00-908 Warsaw, Poland*

(Received 2 September 2016; published 19 January 2017)

High-resolution birefringence (Δn) measurements are carried out to probe the critical behavior at the smectic-*A*–smectic-*C* (Sm-*A*–Sm-*C*) phase transition in a binary system. The critical behavior of this transition is explored with the aid of a differential quotient extracted from the Δn values. The results obtained reveal that the Sm-*A*–Sm-*C* and nematic–smectic-*A* (*N*–Sm-*A*) transitions exhibit nonuniversal behaviors with effective exponents lying between the tricritical and three-dimensional *XY* values and follow two distinctly different curves with decreasing width of the Sm-*A* and *N* phases, respectively. The origin of such critical behavior is a unique feature for the respective phase transitions.

DOI: 10.1103/PhysRevE.95.012705

Classical liquid crystal phases are characterized by broken symmetries and may be utilized to explore the complex and beautiful relationship in nature between symmetry and spatial dimensionality at phase transitions. The smectic-*A* (Sm-*A*) and smectic-*C* (Sm-*C*) phases can be described as orientationally ordered fluids with quasi-long-range one-dimensional mass density waves either parallel (Sm-*A*) or inclined (Sm-*C*) to the unique orientational axis. The transition between the Sm-*A* and Sm-*C* phases involves the breaking of a continuous rotational symmetry. Proposing the order parameter associated with the Sm-*A*–Sm-*C* transition to be $\Psi = \theta \exp(i\phi)$, where θ is the tilt angle of the director with respect to the smectic layer normal and ϕ is an azimuthal angle, de Gennes has predicted that this transition can be continuous and is expected to belong to the three-dimensional (3D) *XY* universality class ($d = 3$ and $n = 2$) [1].

Early experimental studies reveal classical mean-field behavior and can be well described by the extended mean-field model [2]. There are also several examples in which the heat capacity shows Landau behavior including tricritical appearance [3], while in some other cases, clear deviation from the mean-field character has also been observed, exhibiting either a 3D *XY* [4] or Gaussian tricritical [5] nature. Therefore, the question that arises is why certain compounds show mean-field behavior while others critical behavior. The justification for the absence of critical fluctuation for most of the Sm-*A*–Sm-*C* transition can be explained in terms of the Ginzburg criterion, i.e., true critical behavior is expected only when $|\tau| < \tau_G$, where τ is the reduced temperature and τ_G is the Ginzburg temperature. Safinya *et al.* showed that due to the large bare correlation lengths, as obtained from x-ray studies [6], the Ginzburg criterion yields $\tau_G \sim 10^{-5}$. Since the Sm-*C* ordering is apparently not driven by long-range interaction and the Sm-*A*–Sm-*C* transition is not at or above the upper critical dimensionality ($d = 4$ for the *XY* universality class), mean-field theory is not applicable for the exact nature of this transition [7]. However, Huang and Lien [8] and Prasad *et al.* [9] indicated the possibility of observing a first-order or tricritical behavior of this transition by reduction of the Sm-*A* temperature range.

Recently, experimental verification of the crossover phenomena from 3D *XY* to tricritical behavior by decreasing the nematic (*N*) temperature range has been found to be quite successful in the *N*–Sm-*A* phase transition [10,11]. Therefore, it is quite plausible to expect that occurrence of such crossover from 3D *XY* to tricritical and thereafter to first-order behavior seems to be related to the width of the Sm-*A* temperature range [8,9]. Thus the discovery of a suitable system that manifests critical fluctuations associated with the Sm-*A*–Sm-*C* transition is very important. Such a situation has been reported for a few phenyl pyrimidine compounds [12] and also in azoxy-4,4′-bi-undecyl-α-methyl cinnamate [13] as well as some chiral systems [14]. As light is sensitive to the average molecular direction, probably optical measurements are accurate enough to allow for a discussion about the nature of the Sm-*A*–Sm-*C* phase transition. In fact, a nearly tricritical behavior has recently been reported by analyzing the Δn data near the Sm-*A*–Sm-*C* transition in a phenyl pyrimidine compound [15]. We have therefore undertaken high-resolution birefringence measurements to test the possibility of crossover behavior from nearly tricritical to 3D *XY* critical nature near the Sm-*A*–Sm-*C* transition by reducing the Sm-*A* temperature range. In this paper it is shown that the transitional behavior is really critical over the reduced temperature range $2 \times 10^{-4} - 3 \times 10^{-3}$ estimated within 1 K from the transition.

In the present work we report the results on a high-resolution temperature scanning measurement of Δn in a binary system consisting of the second and seventh homologs of the 5-alkyloxy-2-(4-nonyloxy-phenyl) pyrimidine series. A temperature scanning measurement of the optical birefringence has been accomplished by probing the phase retardation $\Delta\phi$ of a laser beam ($\lambda = 532\,\text{nm}$) transmitted through a planar aligned liquid-crystal-filled cell. The birefringence was calculated from the measured normalized intensity and has been described in detail in Ref. [11].

The phase diagram presented in Fig. 1 has been constructed by optical microscopy. Eight mixtures of the binary system (PhP1 + PhP2) were prepared having molar concentrations

---

[*] Corresponding author: mkdnbu@yahoo.com

©2017 American Physical Society

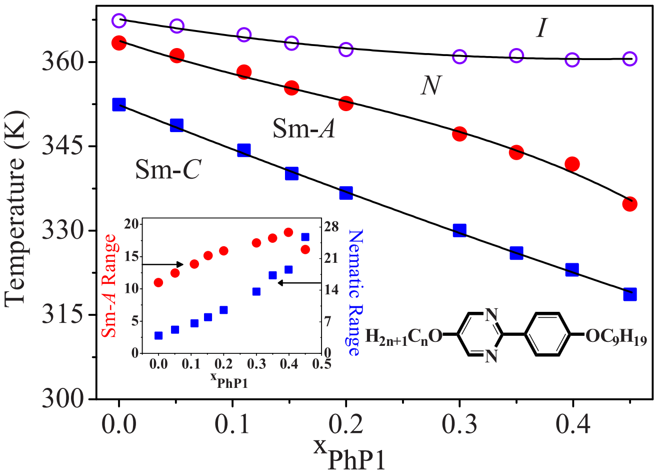

FIG. 1. Partial phase diagram of the binary system comprised of PhP2 and PhP1. Here x_{PhP1} denotes the mole fraction of PhP1; I: isotropic phase; N: nematic phase; Sm-A: smectic-A phase; Sm-C: smectic-C phase; ○: isotropic to nematic transition temperature; ●: nematic to smectic-A transition temperature; ■: smectic-A to smectic-C transition temperature; The structure of the PhP compound is shown. For PhP1, $n = 2$; Crystal (359.7 K) N (363.5 K) I; For PhP2, $n = 7$; Crystal (330 K) Sm-C (352.45 K) Sm-A (363.5 K) N (367.55 K) I. The Inset shows the concentration dependence of the Sm-A and nematic ranges for the present system. Solid lines are drawn to guide the eye.

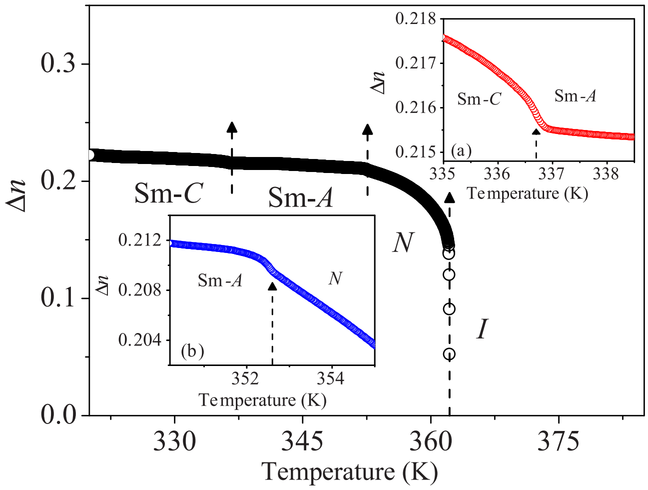

FIG. 2. Temperature dependence of birefringence data for the mixture $x_{\mathrm{PhP1}} = 0.2$. Vertical arrows show the $I-N$, N–Sm-A, and Sm-A–Sm-C phase transitions for the mixtures. In the insets variation of birefringence in the vicinity of the Sm-A–Sm-C transition [inset (a)] and N–Sm-A transition [inset (b)] has been presented.

ranging between 0.05 and 0.45 of PhP1. The variation of the nematic and Sm-A ranges against molar concentration is also presented in the inset of Fig. 1.

Systematic variations in the N and Sm-A widths have been accomplished by the addition of the second homolog (PhP1) of the same series. The nematic range is found to increase from a value of 4–27 K, whereas the Sm-A range lies between 11and 19 K for the studied mixtures. Therefore, it is expected that the dependence of the effective critical exponent α' on the temperature ratios T_{AC}/T_{NA} and T_{NA}/T_{IN} (where T_{AC} is the Sm-A–Sm-C phase transition temperature, T_{NA} is the N–Sm-A phase transition temperature, and T_{IN} is the isotropic to nematic phase transition temperature) can be investigated more rigorously on a rather broad scale, thus endowing us with the insight into the nature of both the Sm-A to Sm-C and N to Sm-A phase transitions from the same binary system of rodlike liquid crystal molecules. The temperature dependence of the Δn for one representative mixture ($x_{\mathrm{PhP1}} = 0.2$) is shown in Fig. 2. After a discontinuity at the weakly first-order transition from the isotropic phase, the birefringence increases rapidly with decreasing temperature due to the increase of the nematic order parameter. Upon lowering the temperature, an enhancement in Δn takes place at the N–Sm-A phase transition. Such augmentation is possibly due to the smectic like short-range order, building up within the nematic phase close to the N–Sm-A phase transition and consequently causing a further enhancement in the nematic orientational order. Moreover, on entering the low-temperature Sm-C phase there is also a clear and overall increase in Δn due to the Sm-A–Sm-C phase transition. This may be due to the fact that the molecular long axis in the Sm-C phase of the surface aligned (planar cell of thickness 7.7 μm) bulk sample is oriented parallel to the aligning surface and the layers are tilted with respect to the surface alignment, which causes an enhancement in the orientational order. We have obtained very well defined Δn curves in the near vicinity of the transition temperatures. It has been found that the quantity $-d(\Delta n)/dT$ is related to a specific-heat capacity anomaly [16] and may be utilized to investigate the critical fluctuation associated with a phase transition. Due to the small temperature interval between the successive data points, the numerically determined temperature derivative of Δn is rather scattered. Therefore, it is reasonable to introduce the differential quotient $Q(T)$, defined as [16,17]

$$Q(T) = -\frac{\Delta n(T) - \Delta n(T_{AC})}{T - T_{AC}}, \qquad (1)$$

where $\Delta n(T_{AC})$ is the birefringence value at T_{AC}, as obtained by differentiating the temperature dependence of Δn. The $Q(T)$ data as obtained have been analyzed in detail with the following renormalization-group expression including the correction-to-scaling terms [17,18]:

$$Q(T) = A^{\pm}|\tau|^{-\alpha'}(1 + D^{\pm}|\tau|^{\Delta}) + E(T - T_{AC}) + B, \qquad (2)$$

where $\tau = (T - T_{AC})/T_{AC}$ is the reduced temperature and the superscripts ± denote those above and below T_{AC}, $A^{\pm}$ presents the critical amplitudes, α' is the critical exponent similar to the specific-heat critical exponent α, $D^{\pm}$ are the coefficients of the first correction-to-scaling terms, and the correction-to-scaling exponent Δ has been taken to be fixed at 0.5 [18]. The term $E(T\text{–}T_{AC})$ corresponds to a temperature-dependent part of the regular background, while B is a constant giving the combined critical and regular backgrounds. Data very close to the transition are excluded from the fitting due to experimental uncertainty and sample inhomogeneity. An overview of the temperature-dependent variation of $Q(T)$ for pure PhP2 and eight different mixtures in the vicinity of the

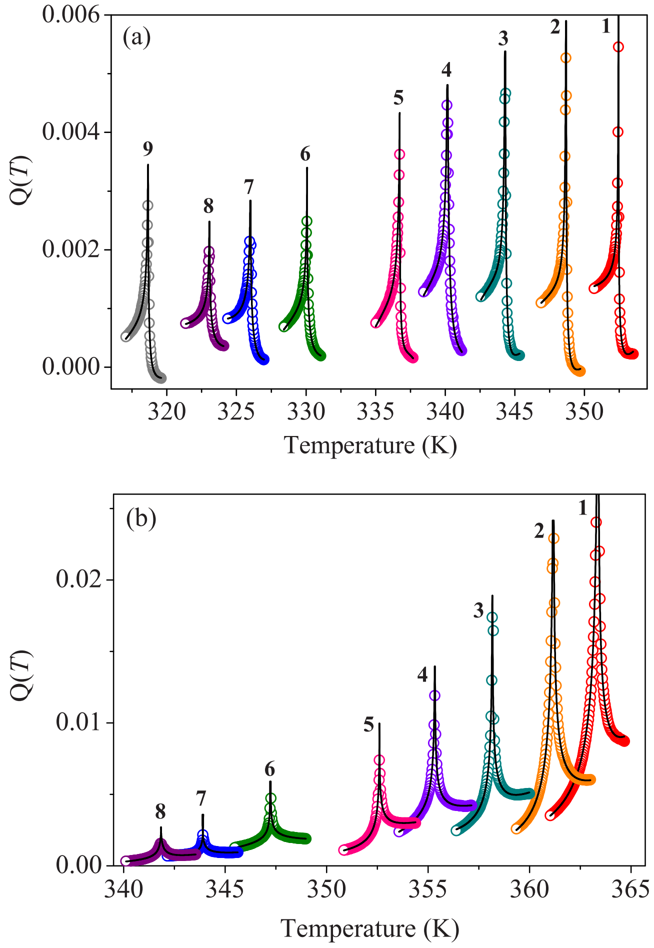

FIG. 3. Temperature dependence of $Q(T)$ in the vicinity of the (a) Sm-A–Sm-C transition and (b) N–Sm-A transition in mixtures of PhP1 + PhP2. 1: $x_{\text{PhP1}} = 0.0$; 2: $x_{\text{PhP1}} = 0.05$; 3: $x_{\text{PhP1}} = 0.1$; 4: $x_{\text{PhP1}} = 0.15$; 5: $x_{\text{PhP1}} = 0.2$; 6: $x_{\text{PhP1}} = 0.3$; 7: $x_{\text{PhP1}} = 0.35$; 8: $x_{\text{PhP1}} = 0.4$; 9: $x_{\text{PhP1}} = 0.45$.

TABLE I. Results corresponding to the best fit for $Q(T)$ near the Sm-A–Sm-C phase transition obtained in accordance with Eq. (2) and related χ_v^2 values associated with the fits.

x_{PhP1}	A^-/A^+	D^-/D^+	α'	χ_v^2
0	1.301 ± 0.014	1.01 ± 0.05	0.476 ± 0.007	1.19
0.05	1.200 ± 0.011	1.00 ± 0.03	0.397 ± 0.006	1.24
0.10	1.080 ± 0.018	0.99 ± 0.05	0.321 ± 0.017	1.17
0.15	1.017 ± 0.098	0.94 ± 0.03	0.237 ± 0.011	1.19
0.20	0.979 ± 0.062	0.93 ± 0.04	0.193 ± 0.007	1.25
0.30	0.911 ± 0.006	0.91 ± 0.03	0.136 ± 0.002	1.13
0.35	0.930 ± 0.002	0.91 ± 0.02	0.089 ± 0.007	1.17
0.40	0.907 ± 0.011	0.91 ± 0.03	0.040 ± 0.006	1.15
0.45	0.936 ± 0.018	0.86 ± 0.06	0.152 ± 0.005	1.08

Sm-A–Sm-C phase transition is shown in Fig. 3(a). The $Q(T)$ data exhibit a noticeable divergent character on both sides of the transition temperature, involving an asymmetry between the $Q(T)$ wings in the Sm-A and Sm-C phases. In particular, the existence of such divergent behavior above the transition temperature clearly indicates that this transition is not of the mean-field type. As both the compounds were chosen from the same homologous series, no Fisher renormalization [19] of the critical exponent has been observed even for nearly tricritical compositions. The fits to Eq. (2) over the range $\tau = 3 \times 10^{-3}$ are displayed as solid lines, while the corresponding fit values are presented in Table I. The reduced error functions χ_v^2, which have been found to be within 1.08–1.25, signify consistent fits.

In an attempt to analyze the critical anomaly associated with the N–Sm-A phase transition the above-discussed procedure has also been used [11]. Here $\Delta n(T_{AC})$ is replaced by $\Delta n(T_{NA})$, while T_{AC} is changed to T_{NA}. The values of the fit parameters as extracted from the fit process are gathered in Table II. The results of fits over the range $\tau = 5 \times 10^{-3}$ represent the $Q(T)$ data well [Fig. 3(b)], as indicated by the χ_v^2 values. Moreover, the critical region for each mixture at the Sm-A–Sm-C phase transition is quite small compared to that for the N–Sm-A phase transition.

The variation of the extracted critical exponent α' values for the present investigated mixtures including that for the pure PhP2 against the temperature ratios (i.e., T_{NA}/T_{IN} and T_{AC}/T_{NA}) is illustrated in Fig. 4. Nonuniversal values have been observed for the critical exponent α' and hence indicate a crossover character for both the N–Sm-A and Sm-A–Sm-C phase transitions. The present results confirm that the width of the N and Sm-A temperature ranges plays an important role in deciding the nature of both the N–Sm-A and the Sm-A–Sm-C phase transitions.

The magnitude of the anomaly in $Q(T)$ decreases significantly as the N and Sm-A ranges grows, showing that thermal fluctuations associated with the $Q(T)$ anomaly are very sensitive to the saturation of both the N and the Sm-A order. The overall behavior between α' and T_{NA}/T_{IN} from the tricritical point (TCP) towards approaching the 3D XY value is in good agreement with the previous reports on the N–Sm-A phase transitions [11,20–25], which are also included in Fig. 4.

In the vicinity of the Sm-A–Sm-C phase transition, the measured value of critical exponent α' for pure PhP2 as reported by Chakraborty *et al.* [15] was 0.48 ± 0.02 and the repeated measurement for different cell thickness yielded 0.476 ± 0.007. With increasing PhP1 concentration, α' decreases monotonically from 0.476 ± 0.007 for PhP2 to 0.04 ± 0.006 for $x_{\text{PhP1}} = 0.40$, i.e., the yielded values of the effective critical exponent α', characterizing the critical fluctuation at this transition, have appeared to be in between those predicted

TABLE II. Results corresponding to the best fit for $Q(T)$ near the N–Sm-A phase transition obtained in accordance with Eq. (2) and related χ_v^2 values associated with the fits.

x_{PhP1}	A^-/A^+	D^-/D^+	α'	χ_v^2
0	1.630 ± 0.029	0.99 ± 0.04	0.462 ± 0.002	1.29
0.05	1.521 ± 0.052	0.99 ± 0.01	0.425 ± 0.007	1.11
0.10	1.417 ± 0.036	1.00 ± 0.01	0.387 ± 0.011	1.36
0.15	1.368 ± 0.107	1.00 ± 0.01	0.345 ± 0.005	1.02
0.20	1.450 ± 0.088	1.00 ± 0.01	0.303 ± 0.004	1.12
0.30	1.053 ± 0.038	1.01 ± 0.01	0.188 ± 0.003	1.21
0.35	0.970 ± 0.017	1.00 ± 0.01	0.084 ± 0.001	1.18
0.40	0.983 ± 0.010	1.01 ± 0.03	0.053 ± 0.001	1.46

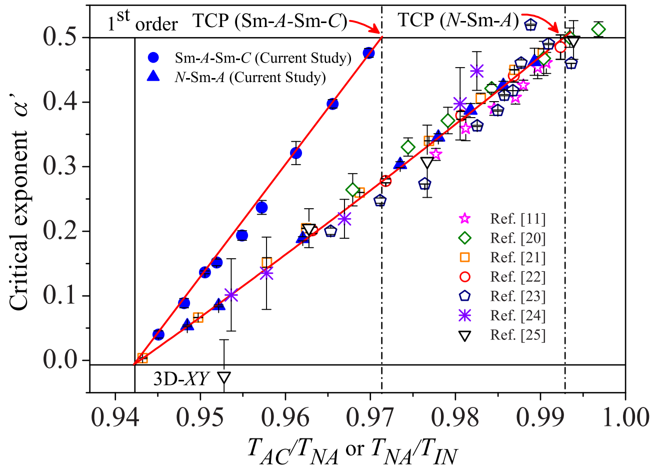

FIG. 4. Variation of effective critical exponent α' with T_{NA}/T_{IN} for the N–Sm-A transition and T_{AC}/T_{NA} for the Sm-A–Sm-C transition. The vertical dash-dotted lines and solid line correspond to the TCP and 3D XY limit, respectively. The solid (red) lines are linear fit to the data.

by the 3D XY, i.e., $\alpha_{XY} = -0.007$, and tricritical, i.e., $\alpha = 0.5$, values. The dependence of this transition on the Sm-A range has also qualitatively been observed by others [8,9].

An extrapolation of the linear fit to the extracted α' values yield a tricritical behavior (i.e., $\alpha' = 0.5$) for the T_{AC}/T_{NA} ratio of 0.972, which is quite low in comparison to that obtained for a similar temperature ratio ($T_{NA}/T_{IN} = 0.992$) at the N–Sm-A phase transition. However, the linear fit to the α' data yields a T_{AC}/T_{NA} value of 0.942 corresponding to the 3D XY point, which is found to be very close to the McMillan ratio (T_{NA}/T_{IN}) for the N–Sm-A phase transition.

It should be mentioned here that this crossover of α' gives rise to characteristic behavior regarding the amplitude ratio (A^-/A^+) and the magnitude of the first-order correction-to-scaling terms (D^-/D^+). In the case of the Sm-A–Sm-C phase transition the A^-/A^+ values are in the range between 1.301 and 0.907 (from the extrapolation 1.39 for the TCP and 0.954 for the 3D XY point) and the first-order correction-to-scaling ratio is between 1.01 and 0.86 (from the extrapolation 1.05 for the TCP and 0.89 for the 3D XY point), while for the N–Sm-A phase transition, although A^-/A^+ varies from 1.63 to 0.97 (from the extrapolation 1.67 for the TCP and 0.99 for the 3D XY point), D^-/D^+ remains nearly unity. The theory for the 3D XY universality class predicts an amplitude ratio $A^-/A^+ = 0.971$ and $D^-/D^+ \approx 1$, while for the TCP the theoretical amplitude ratio $A^-/A^+ = 1.6$ and $D^-/D^+ \approx 1$. Therefore, from our observation, it is clear that the studied mixtures exhibit nonuniversal behaviors with effective exponents lying between the 3D XY and tricritical limits.

It may be worth mentioning that recently, another binary mixture of the rodlike 4′-heptyloxy-4-cyanobiphenyl and the hockey-stick-shaped compound [4-(3-n-decyloxy-2-methyl-phenyliminomethyl) phenyl 4-n-dodecyloxy cinnamate] exhibit critical behavior and has also been found to show a tricritical point around $T_{AC}/T_{NA} = 0.97$ with a quite broad tricritical range [26].

In conclusion, we believe that our result may close the controversy on the nature of the Sm-A–Sm-C transition. The nonuniversal behavior of this transition with either very weak first-order or second-order nature with Gaussian tricritical or crossover from 3D XY critical to tricritical behavior can now be clearly explained on the basis of the width of the Sm-A temperature range linked with the Sm-A–Sm-C phase transition. However, mean-field tricritical or mean-field 3D XY behavior is only an approximation where the true critical region remains inaccessible. Moreover, it seems that the origin of such critical behavior is perhaps a unique feature for both the N–Sm-A and the Sm-A–Sm-C phase transitions for all the compounds since they are observed to follow two distinctly different linear curves as shown in Fig. 4.

We gratefully acknowledge financial support from the Department of Science and Technology, New Delhi (Project No. SB/EMEQ-290/2013). S.C. is grateful to the DST, New Delhi for support through the award of a project assistantship.

---

[1] P. G. de Gennes, Mol. Cryst. Liq. Cryst. **21**, 49 (1973).

[2] C. C. Huang and J. M. Viner, Phys. Rev. A **25**, 3385 (1982); M. Meichle and C. W. Garland, *ibid.* **27**, 2624 (1983); P. Das, K. Ema, and C. W. Garland, Liq. Cryst. **4**, 205 (1989).

[3] H. Y. Liu, C. C. Huang, C. Bahr, and G. Heppke, Phys. Rev. Lett. **61**, 345 (1988); T. Chan, C. Bahr, G. Heppke, and C. W. Garland, Liq. Cryst. **13**, 667 (1993); R. J. Birgeneau, C. W. Garland, A. R. Kortan, J. D. Litster, M. Meichle, B. M. Ocko, C. Rosenblatt, L. J. Yu, and J. Goodby, Phys. Rev. A **27**, 1251 (1983).

[4] K. Ema, J. Watanabe, A. Takagi, and H. Yao, Phys. Rev. E **52**, 1216 (1995).

[5] K. Ema, A. Takagi, and H. Yao, Phys. Rev. E **55**, 508 (1997); T. Stoebe, L. Reed, M. Veum, and C. C. Huang, *ibid.* **54**, 1584 (1996).

[6] C. R. Safinya, M. Kaplan, J. Als-Nielsen, R. J. Birgeneau, D. Davidov, J. D. Litster, D. L. Johnson, and M. E. Neubert, Phys. Rev. B **21**, 4149 (1980).

[7] A. Altland and B. Simons, *Condensed Matter Field Theory* (Cambridge University Press, Cambridge, 2010).

[8] C. C. Huang and S. C. Lien, Phys. Rev. A **31**, 2621 (1985).

[9] S. K. Prasad, V. N. Raja, D. S. Rao, G. G. Nair, and M. E. Neubert, Phys. Rev. A **42**, 2479 (1990).

[10] K. J. Stine and C. W. Garland, Phys. Rev. A **39**, 3148 (1989).

[11] A. Chakraborty, S. Chakraborty, and M. K. Das, Phys. Rev. E **91**, 032503 (2015).

[12] L. Reed, T. Stoebe, and C. C. Huang, Phys. Rev. E **52**, R2157 (1995); G. S. Iannacchione, C. W. Garland, P. M. Johnson, and C. C. Huang, Liq. Cryst. **26**, 51 (1999).

[13] Y. Galerne, Phys. Rev. A **24**, 2284 (1981).

[14] K. Ema and H. Yao, Phys. Rev. E **57**, 6677 (1998), and references therein.

[15] A. Chakraborty, S. Chakraborty, and M. K. Das, Physica B **479**, 90 (2015).

[16] M. C. Çetinkaya, S. Yildiz, H. Özbek, P. Losada-Pérez, J. Leys, and J. Thoen, Phys. Rev. E **88**, 042502 (2013).

[17] S. Erkan, M. Çetinkaya, S. Yildiz, and H. Özbek, Phys. Rev. E **86**, 041705 (2012).

[18] C. W. Garland, in *Liquid Crystals: Experimental Study of Physical Properties and Phase Transitions*, edited by S. Kumar (Cambridge University Press, Cambridge, 2001).

[19] M. E. Fisher, Phys. Rev. **176**, 257 (1968).

[20] S. K. Sarkar and M. K. Das, J. Mol. Liq. **199**, 415 (2014).

[21] S. K. Sarkar, A. Chakraborty, and M. K. Das, Liq. Cryst. **43**, 22 (2016).

[22] S. Chakraborty, A. Chakraborty, and M. K. Das, J. Mol. Liq. **219**, 608 (2016).

[23] G. Cordoyiannis, C. S. P. Tripathi, C. Glorieux, and J. Thoen, Phys. Rev. E **82**, 031707 (2010).

[24] C. W. Garland and G. Nounesis, Phys. Rev. E **49**, 2964 (1994).

[25] Y. Sasaki, K. Ema, K. V. Le, H. Takezoe, S. Dhara, and B. K. Sadashiva, Phys. Rev. E **83**, 061701 (2011).

[26] S. Chakraborty and M. K. Das (unpublished).